Estimation of the Hemodynamic Response of fMRI Data Using RBF Neural Network

Huaien Luo and Sadasivan Puthusserypady*, *Senior Member, IEEE*

***Abstract*—Functional magnetic resonance imaging (fMRI) is an important technique for neuroimaging. The conventional system identification methods used in fMRI data analysis assume a linear time-invariant system with the impulse response described by the hemodynamic responses (HDR). However, the measured blood oxygenation level-dependent (BOLD) signals to a particular processing task (for example, rapid event-related fMRI design) show nonlinear properties and vary with different brain regions and subjects. In this paper, radial basis function (RBF) neural network (a powerful technique for modelling nonlinearities) is proposed to model the dynamics underlying the fMRI data. The equivalence of the proposed method to the existing Volterra series method has been demonstrated. It is shown that the first- and second-order Volterra kernels could be deduced from the parameters of the RBF neural network. Studies on both simulated (using Balloon model) as well as real event-related fMRI data show that the proposed method can accurately estimate the HDR of the brain and capture the variations of the HDRs as a function of the brain regions and subjects.**

***Index Terms*—Event-related design, functional magnetic resonance imaging (fMRI), hemodynamic response (HDR), neural network, radial basis functions (RBF), Volterra kernels.**

I. Introduction

FUNCTIONAL magnetic resonance imaging (fMRI) is a neuroimaging technique to understand the functioning of the human brain in response to stimuli. Through the analysis of the variations of blood oxygenation level-dependent (BOLD) signals [1] measured by the fMRI equipment, activated regions of the human brain under different perceptual, motor or cognitive conditions can be detected. Neurons in the activated areas of the brain need more oxygen for their functioning than the inactivated ones and this induces the oxygen supply to increase and exceed the demand for oxygen. This imbalance between the supply and demand of oxygen results in a substantial drop in the deoxyhemoglobin content of the venous blood. The magnetic resonance (MR) signal is sensitive to this change because of the paramagnetic property of deoxyhemoglobin. The reduction of deoxyhemoglobin concentration leads to an increase of MR signal—known as the BOLD effect [2], [3]. The changes in the intensity of the measured BOLD signal is dependent on the total amount of deoxyhemoglobin, which is influenced by the cerebral blood volume (CBV), cerebral blood flow (CBF) and the cerebral metabolic rate of oxygen (CMRO_2) [4]. Therefore, the measured BOLD signal can be viewed as a complex function of the physiological changes related to different experimental tasks.

There are mainly two types of fMRI experimental designs: *blocked* and *event-related* [3]. In the blocked design, a series of events in one condition is presented consecutively for an extended period of time. The signal measured during one block is then compared with other blocks of different task conditions. Event-related designs, on the other hand, present discrete, short-duration trial events one at a time rather than together in a block. For both designs, dynamic MR images are collected covering the whole or part of the brain, with relatively low resolution compared to the conventional anatomical (or structural) images. The fMRI data is a 4-D spatio-temporal dataset, which is obtained by repeatedly scanning the images of the chosen volume of the brain with a repetition time (TR) [3].

Many methods (linear and nonlinear) have been proposed to analyze and model the complex fMRI data. The general linear model (GLM) assumes the linearity of hemodynamic response (HDR) and regresses the fMRI signals onto the regressors constructed by the convolution of the canonical hemodynamic response function (HRF) and the experimental stimuli [5], [6]. However, considering that the HDR varies with different brain regions and subjects [7], if the presumed waveform of the HRF is different from the actual HDR, we may fail to detect the activities of the brain. To capture the small variations of the HDR, basis functions were proposed to model the HDR in GLM [8]. These basis functions composed of a combination of regressors (the canonical HRF, its temporal and dispersion derivatives) span a subspace to capture the variations of the HDR. However, in this method, these regressors can only capture small variations of the HDR and for large variations, it may underestimate or even fail to capture the diversities of the HDR. Thus, a flexible HDR modelling is preferred to deal with the variations of HDR.

The fMRI signals also exhibit nonlinear properties especially in the rapid event-related fMRI experiments when the stimulation duration or interstimulus intervals (ISI) is less than 4–6 s [9]–[11]. These nonlinearities arise from both vascular and neuronal levels [12]. Several advanced nonlinear models have been proposed to analyze such fMRI data. The nonlinear dynamics of the BOLD signal is first described by the Balloon model, which is a physiologically derived model introduced by Buxton *et al.* [14]. The couplings between blood flow and blood

Manuscript received June 22, 2006; revised November 5, 2006. This work was supported in part by the National University of Singapore, Singapore, under Faculty Research Grant R-263-000-360-112. *Asterisk indicates corresponding author.*

H. Luo is with the Department of Electrical and Computer Engineering, National University of Singapore, Singapore 117576, Singapore (e-mail: g0305766@nus.edu.sg).

*S. Puthusserypady is with the Department of Electrical and Computer Engineering, National University of Singapore, 4 Engineering Drive 3, Singapore 117576, Singapore (e-mail: elespk@nus.edu.sg).

Color versions of one or more of the figures in this paper are available online at http://ieeexplore.ieee.org.

Digital Object Identifier 10.1109/TBME.2007.900795

oxygen concentration changes on a biological level are incorporated into this nonlinear state-space model. The interpretability of the parameters in the Balloon model makes it a suitable model to understand the nonlinear mechanisms underlying the BOLD effect. The Balloon model has undergone several extensions since its introduction. Friston *et al.* extended the original model to include a linear interaction between synaptic activity (or electrophysiology) and the microvascular control system [15]. Recently, Buxton *et al.* incorporated CMRO_2 and neural activity as new variables in the Balloon model and described the steps linking an external stimulus to the measured BOLD and CBF responses [16]. These physiologically derived nonlinear models have many advantages such as meaningful interpretations of the parameters. However, it is not an easy task to estimate the parameters in such nonlinear models. The nonphysiological models described in the following sections, on the other hand, are easier to implement and more flexible for a better mapping of the input to the output if the signal is highly nonlinear.

The Volterra series method, which can model any dynamical input-output system, was also proposed to analyze and estimate the HDR using the first- and second-order Volterra kernels [13]. Though this method represents the nonlinear properties of the BOLD signal, it has a number of limitations. To get a better representation of the dynamical system, higher order Volterra kernels are required. However, the inclusion of higher order Volterra kernels requires fitting a large number of parameters. Especially, the number of terms in the kernels of the series increases exponentially with the order of the series. Due to these difficulties and complexity in identifying the higher order kernels, an alternative, yet efficient method to estimate the kernels in the Volterra series is desired.

In this paper, a novel method of the estimation of the kernels is proposed. This method describes the nonlinear dynamics of the fMRI hemodynamic response using the radial basis function (RBF) neural network. It is known that neural network could approximate any continuous functions to any degree of accuracy due to its universal approximation property. Modelling the fMRI system as nonlinear and dynamical, the RBF neural network is capable of regressing nonlinearly the BOLD signal to the external stimuli. Additionally, the relationship between the parameters of the RBF neural network and Volterra kernels is provided and the HDR could easily be estimated from the parameters of the neural network. This provides an efficient method to calculate the large number of parameters in the Volterra series kernels.

The rest of the paper is organized as follows. Section II introduces the Volterra series model, Balloon model and RBF neural network method for fMRI data analysis. The equivalence of the proposed neural network method to the Volterra series method is also demonstrated in this section. Results of the simulation studies are discussed in Section III followed by the concluding remarks in Section IV.

II. Methods

A. Volterra Series Model

The measured fMRI signal, $y(n)$ $(n = 0, 1, \ldots, N-1)$, can be described as a nonlinear convolution of the stimulus function, $u(n)$, with the Volterra kernels where the nonlinear properties are captured by the higher order kernels. The Volterra series method to model the fMRI signal does not include the variables such as blood volume, blood flow, oxygenation, etc., introduced in the Balloon model which makes the parameters in the model easier to estimate. When the BOLD signal is represented in the form of a finite (second-order) Volterra series, the output BOLD signal, $y_B(n)$, can be written as a function of the input stimulus, $u(n)$, as

$$y_B(n) = a_0 + \sum_{i=0}^{P} a_1(i)u(n-i) + \sum_{i=0}^{P}\sum_{j=0}^{P} a_2(i,j)u(n-i)u(n-j) \quad (1)$$

where the length of the kernels is $(P+1)$. The constant a_0 is the zeroth-order kernel. The coefficients $a_1(\cdot)$ are the first-order kernels which relate the output as the weighted sum of the present and the recent past inputs; these coefficients represent the HDR in fMRI. The coefficients $a_2(\cdot,\cdot)$ in the above equation are the second-order Volterra kernels which represent the output as the interactions between the present and/or the recent past inputs at different time points. It can be observed that the kernels $a_2(i,j) = a_2(j,i), \forall i,j$, due to the symmetry property. The input stimulus $u(n)$ represents the timing of the external stimuli with the value equal to "1" when the stimulus is present (ON) and "0" when the stimulus is absent (OFF). For the blocked design, the stimulus function $u(n)$ is a boxcar function and for event-related design, it is a series of impulses with unit amplitudes at the time points where the stimuli are presented [2].

The measured fMRI signal, $y(n)$, is a noise corrupted version of the BOLD signal, $y_B(n)$, and can be represented as

$$y(n) = y_B(n) + e(n) \quad (2)$$

where $e(n)$ is the additive noise. The solution to the Volterra series model could be obtained using a least-square method (assuming the noise to be white Gaussian). Substituting (1) into (2), it can be represented in the matrix form as

$$\mathbf{y} = \mathbf{\Phi x} + \mathbf{e} \quad (3)$$

where $\mathbf{y} = [y(P), \ldots, y(N-1)]^T$ is the measured signal of dimension $(N-P)\times 1$; $\mathbf{e} = [e(P), \ldots, e(N-1)]^T$ is the noise vector with the same dimension. The coefficient vector $\mathbf{x}$ [of dimension $(L\times 1)$] and the matrix $\mathbf{\Phi}$ [of dimension $(N-P)\times L$] are shown in (4) and (5), respectively, shown at the top of the next page. Here, N is the total number of measured output samples, and $L = (P+3)(P+2)/2$ considering the symmetry of the coefficients of $a_2(\cdot,\cdot)$. The least-squares (LS) estimate of the coefficients $(\hat{\mathbf{x}})$ is given by

$$\hat{\mathbf{x}} = (\mathbf{\Phi}^T\mathbf{\Phi})^{-1}\mathbf{\Phi}^T\mathbf{y}. \quad (6)$$

It needs to be noted that for the event-related fMRI design, the matrix $\mathbf{\Phi}$ may become singular because the stimuli function $u(n)$ contains only zeroes and ones, which may cause some columns in $\mathbf{\Phi}$ to be zero. Additionally, the Volterra series model

$$\mathbf{x} = [a_0, a_1(0), \ldots a_1(P), a_2(0,0), a_2(0,1), \ldots a_2(P,P)]^T \tag{4}$$

$$\mathbf{\Phi} = \begin{pmatrix} 1 & u(P) & \ldots & u(0) & u^2(P) & u(P)u(P-1) & \ldots & u^2(0) \\ 1 & u(P+1) & \ldots & u(1) & u^2(P+1) & u(P+1)u(P) & \ldots & u^2(1) \\ \vdots & \vdots & \ddots & \vdots & \vdots & \vdots & \ddots & \vdots \\ 1 & u(N-1) & \ldots & u(N-P-1) & u^2(N-1) & u(N-1)u(N-2) & \ldots & u^2(N-P) \end{pmatrix} \tag{5}$$

needs to specify the order to which the representation is carried out. Inclusion of higher orders in Volterra series allows a better representation of the dynamical system under study. However, since all the related kernel parameters need to be estimated together if using LS method, inclusion of higher order Volterra series causes the number of parameters to be estimated increasing exponentially with the order. For example, if the BOLD signal with $\mathrm{TR} = 1$ s is modelled using Volterra series of order 3, the number of parameters to be estimated is more than 4000 if the kernels are to capture the temporal properties within 20 s after stimuli. Therefore, an efficient and accurate method for the calculation of the Volterra kernels is desired. In the following section, such a method (the RBF neural network method) is provided. Especially, the calculation of Volterra series kernels is derived from the parameters of the RBF neural network. Compared to the Volterra series method estimated by LS, the proposed method could model the systems nonlinearity even when higher order kernels are needed. Also since the kernel parameters are estimated independently, the lower order Volterra kernels could still be accurately calculated even when the higher order Volterra kernels are not estimated.

B. Neural Networks Model

Neural network, a powerful method for modelling nonlinear systems [17], is used in this work to describe the nonlinear dynamics of HDR [18], [19]. The present and the recent past inputs are applied to the neural network and the BOLD signal $y(n)$ from a specific voxel is used as the desired output signal. Thus, the measured BOLD signal can be expressed as the nonlinear function of the input stimulus as follows:

$$\hat{y}(n) = F^{NN}(\mathbf{u}(n)) \tag{7}$$

where $\mathbf{u}(n) = [u(n), u(n-1), \ldots, u(n-P)]^T$ is the input vector of dimension $(P+1)\times 1$ formed by the present and recent past inputs with the maximum delay P. The output $\hat{y}(n)$ is a nonlinear function (denoted by F^{NN}) of the input vector $\mathbf{u}(n)$. This functional mapping is realized by the RBF network as shown in Fig. 1. The universal approximation property and straightforward computation using linearly weighted combination of single layer neurons have made RBF network a good choice in the dynamic reconstruction applications such as the one dealt in this paper. Moreover, the RBF network has a simpler structure (one hidden layer) and easier to implement compared to the multilayer perceptrons (MLP) neural network which may require more than one hidden layers and more time for learning the underlying nonlinearity.

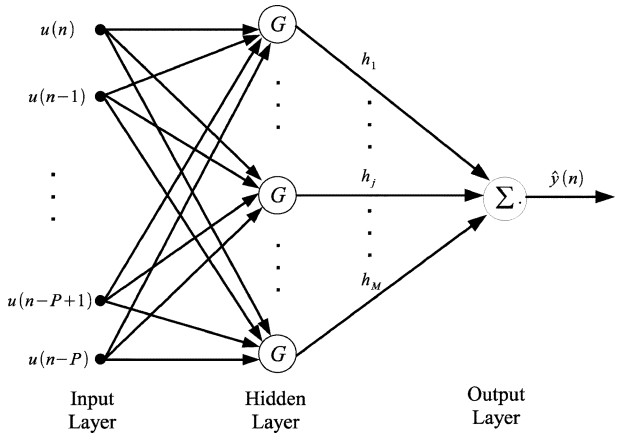

Fig. 1. The structure of the RBF neural network.

Suppose there are M hidden units in the RBF network, then the output $\hat{y}(n)$ of the mapping is taken to be a linear combination of the basis functions, i.e.,

$$\hat{y}(n) = \sum_{i=1}^{M} h_i G(\mathbf{u}(n), \mathbf{c}_i) \tag{8}$$

where h_i $(i = 1, \ldots, M)$ are the weighting coefficients (linear output layer) and $\mathbf{c}_i$ $(i = 1, \ldots, M)$ are the centers of the radial basis functions. Commonly used basis functions are Gaussian functions which are defined as

$$G(\mathbf{u}(n), \mathbf{c}_i) = \exp\Big(-\frac{1}{\sigma_i^2}\|\mathbf{u}(n) - \mathbf{c}_i\|^2\Big) \tag{9}$$

where σ_i^2 is the variance of the ith Gaussian basis function.

The following subsection presents the equivalence of the RBF network and Volterra series methods. This equivalence could also be generalized to the MLP with simple structures (one hidden layer), whereas this equivalence is not so straightforward for structures with more than one hidden layers.

1) Relation Between RBF Neural Network and Volterra Series: According to (8) and (9), $\hat{y}(n)$ can be written as

$$\begin{aligned} \hat{y}(n) &= \sum_{i=1}^{M} h_i e^{-(\|\mathbf{u}(n)-\mathbf{c}_i\|^2)/\sigma_i^2} \\ &= \sum_{i=1}^{M} h_i e^{-1/\sigma_i^2(\mathbf{u}(n)-\mathbf{c}_i)^T(\mathbf{u}(n)-\mathbf{c}_i)} \\ &= \sum_{i=1}^{M} h_i e^{-1/\sigma_i^2(\mathbf{u}^T(n)\mathbf{u}(n)-2\mathbf{u}^T(n)\mathbf{c}_i+\mathbf{c}_i^T\mathbf{c}_i)} \\ &= \sum_{i=1}^{M} \left(h_i e^{-1/\sigma_i^2\mathbf{c}_i^T\mathbf{c}_i}\right) e^{x_i}. \end{aligned} \tag{10}$$

Here, x_i is defined as

$$x_i = -\frac{1}{\sigma_i^2}(\mathbf{u}^T(n)\mathbf{u}(n) - 2\mathbf{u}^T(n)\mathbf{c}_i) = -\frac{1}{\sigma_i^2}\left(\sum_{j=0}^{P} u^2(n-j) - 2\sum_{j=0}^{P} c_{ij}u(n-j)\right) \quad (11)$$

where $\mathbf{c}_i$ is the ith center and c_{ij} is the jth element of $\mathbf{c}_i$.

According to the Taylor series expansion of e^{x_i} at origin

$$e^{x_i} = \sum_{n=0}^{\infty} \frac{x_i^n}{n!} = 1 + x_i + \frac{1}{2!}x_i^2 + \frac{1}{3!}x_i^3 + \cdots \quad (12)$$

and substituting (12) into (10), we get (13), shown at the bottom of the page. Comparing the above equations with (1), it can be seen that the zeroth-, first-, and second-order Volterra kernels can be deduced as

$$a_0 = h_1 e^{-\mathbf{c}_1^T\mathbf{c}_1/\sigma_1^2} + h_2 e^{-\mathbf{c}_2^T\mathbf{c}_2/\sigma_2^2} + \cdots + h_M e^{-\mathbf{c}_M^T\mathbf{c}_M/\sigma_M^2} \quad (14)$$

$$a_1(i) = 2\left(h_1 e^{-(1/\sigma_1^2)c_1^T c_1}\frac{1}{\sigma_1^2}c_{1i} + h_2 e^{-(1/\sigma_2^2)c_2^T c_2}\frac{1}{\sigma_2^2}c_{2i} + \cdots + h_M e^{-(1/\sigma_M^2)c_M^T c_M}\frac{1}{\sigma_M^2}c_{Mi}\right) \quad (15)$$

$$a_2(i,j) = 2\left(h_1 e^{-(1/\sigma_1^2)c_1^T c_1}\frac{1}{\sigma_1^4}c_{1i}c_{1j} + h_2 e^{-(1/\sigma_2^2)c_2^T c_2}\frac{1}{\sigma_2^4}c_{2i}c_{2j} + \cdots + h_M e^{-(1/\sigma_M^2)c_M^T c_M}\frac{1}{\sigma_M^4}c_{Mi}c_{Mj}\right) - \left(\frac{1}{\sigma_1^2}h_1 e^{-(1/\sigma_1^2)c_1^T c_1} + \frac{1}{\sigma_2^2}h_2 e^{-(1/\sigma_2^2)c_2^T c_2} + \cdots + \frac{1}{\sigma_M^2}h_M e^{-(1/\sigma_M^2)c_M^T c_M}\right)\delta(i-j) \quad (16)$$

$$a_2(j,i) = a_2(i,j), \forall i,j. \quad (17)$$

The above equations build the link between the Volterra series and RBF neural network. This implies that the Volterra kernels can be easily deduced from the parameters of the RBF neural network. It is also easy to extend the neural network method to deduce the coefficients of the third- or higher order Volterra kernels if more terms from the Taylor series are incorporated into the expansion series.

As described in the previous section, the performance of the Volterra series method is determined by the choice of the order of Volterra series. Considering only the lower order Volterra kernels may not capture the dynamical properties of the system well. Inclusion of higher order Volterra kernels, although, could model the dynamical system better, it poses the problem of higher computational complexity in identifying the higher order kernels. Compared to the Volterra series method, the neural network method could model the nonlinear dynamical system well even when the system is highly nonlinear. Besides, to estimate the Volterra kernels using LS method, all the relevant Volterra kernels need to be estimated together and this is difficult when the order of the Volterra kernels included is high. However, using the RBF neural network method, the lower order Volterra kernels can be estimated from the RBF parameters (independently) without the estimation of the higher order kernels. This is useful because for most cases, we are only interested in the lower order Volterra kernels. The proposed neural network method provides an efficient approach to estimate the lower order Volterra kernels and at the same time capture the nonlinearities of the system. In addition, the RBF neural network method avoids the possible singularity problem [$\mathbf{\Phi}$ in (6)] of the LS method.

2) Learning Procedure: The centers $\mathbf{c}_i$ of the radial basis functions are chosen randomly from the training data set and the variances of the basis functions are fixed according to the spread of the centers. For fixed centers $\mathbf{c}_i$ and variance σ_i^2, the aim of the RBF network is to find the weights h_i such that the sum-squared-error is minimized. Considering the noise presented in the data, regularization is required to stabilize the solution [17]. The regularized RBF network gives the following estimates of the weight vector, $\mathbf{h} = [h_1, \ldots, h_M]^T$

$$\mathbf{h} = (\mathbf{G}^T\mathbf{G} + \lambda\mathbf{I})^{-1}\mathbf{G}^T\mathbf{y} \quad (18)$$

$$\hat{y}(n) = \left(h_1 e^{-\mathbf{c}_1^T\mathbf{c}_1/\sigma_1^2} + h_2 e^{-\mathbf{c}_2^T\mathbf{c}_2/\sigma_2^2} + \cdots + h_M e^{-\mathbf{c}_M^T\mathbf{c}_M/\sigma_M^2}\right) + 2\sum_{i=0}^{P}\left(h_1 e^{-(1/\sigma_1^2)c_1^T c_1}\frac{1}{\sigma_1^2}c_{1i} + h_2 e^{-(1/\sigma_2^2)c_2^T c_2}\frac{1}{\sigma_2^2}c_{2i} + \cdots + h_M e^{-(1/\sigma_M^2)c_M^T c_M}\frac{1}{\sigma_M^2}c_{Mi}\right)u(n-i) + 2\sum_{i=0}^{P}\sum_{j=0}^{P}\left(h_1 e^{-(1/\sigma_1^2)c_1^T c_1}\frac{1}{\sigma_1^4}c_{1i}c_{1j} + h_2 e^{-(1/\sigma_2^2)c_2^T c_2}\frac{1}{\sigma_2^4}c_{2i}c_{2j} + \cdots + h_M e^{-(1/\sigma_M^2)c_M^T c_M}\frac{1}{\sigma_M^4}c_{Mi}c_{Mj}\right)u(n-i)u(n-j) + \sum_{j=0}^{P}\left(-\frac{1}{\sigma_1^2}h_1 e^{-(1/\sigma_1^2)c_1^T c_1} - \frac{1}{\sigma_2^2}h_2 e^{-(1/\sigma_2^2)c_2^T c_2} - \cdots - \frac{1}{\sigma_M^2}h_M e^{-(1/\sigma_M^2)c_M^T c_M}\right)u(n-j)^2 + \cdots\cdots \quad (13)$$

where λ is the regularization parameter, $\mathbf{y}$ is the vector representing measured fMRI signal, and $\mathbf{G}$ is an $(N-P)\times M$ interpolation matrix, which is defined as

$$\mathbf{G}=\begin{pmatrix} G(\mathbf{u}(P),\mathbf{c}_1) & \dots & G(\mathbf{u}(P),\mathbf{c}_M) \\ \vdots & \ddots & \vdots \\ G(\mathbf{u}(N-1),\mathbf{c}_1) & \dots & G(\mathbf{u}(N-1),\mathbf{c}_M) \end{pmatrix}. \quad (19)$$

The regularization parameter $\lambda > 0$ controls the balance between fitting the data and regularization. A small value of λ means the data can be fit tightly without causing a large regularization; a large value of λ means a tight fit has to be sacrificed to a smoothing output function.

Here, $\mathbf{h}$ and λ can be estimated through Bayesian learning by iteratively updating the following equations [20]:

$$\mathbf{\Sigma}=\beta^2(\mathbf{G}^T\mathbf{G}+\lambda\mathbf{I})^{-1} \quad (20)$$

$$\hat{\mathbf{h}}=\frac{1}{\beta^2}\mathbf{\Sigma}\mathbf{G}^T\mathbf{y} \quad (21)$$

$$\gamma=M-\frac{\lambda}{\beta^2}\mathrm{trace}(\mathbf{\Sigma}) \quad (22)$$

$$\beta^2=\frac{\|\mathbf{y}-\mathbf{G}\hat{\mathbf{w}}\|^2}{N-\gamma} \quad (23)$$

$$\lambda=\frac{\gamma\beta^2}{\hat{\mathbf{w}}^T\hat{\mathbf{w}}} \quad (24)$$

where β^2 is the estimated variance of the noise.

The reconstructed BOLD signal $\mathbf{y}_B$ is then calculated as

$$\hat{\mathbf{y}}_B=\mathbf{G}\hat{\mathbf{h}}. \quad (25)$$

One advantage of Bayesian learning of RBF neural network is that the cross-validation to find the suitable regularization parameter is not needed, which means that all the training data can be used. This is especially useful in the fMRI time series analysis since the number of the available data points is limited.

C. Balloon Model

The Balloon model is a physiologically inspired model introduced by Buxton *et al.* to describe the dynamics of the BOLD signal [14]. In this paper, the Balloon model is used to generate the simulated BOLD signal. In this section, a brief description of the Balloon model is provided.

The Balloon model is a state-space model which describes the dynamics among blood flow, blood volume and blood oxygen concentration changes. The model is inherently nonlinear and can be used to explain the nonlinearities appearing in the BOLD signals. It is described by the following equations:

$$\begin{cases} \dot{f} &= s \\ \dot{s} &= \epsilon u-k_s s-k_f(f-1) \\ \dot{v} &= \frac{1}{\tau}(f-v^{1/\alpha}) \\ \dot{q} &= \frac{1}{\tau}(f\frac{1-(1-E_0)^{1/f}}{E_0}-v^{1/\alpha-1}q) \\ y_B &= V_0(7E_0(1-q)+2\left(\frac{1-q}{v}\right)+(2E_0-0.2)(1-v)) \end{cases} \quad (26)$$

where f is the CBF, v is the CBV, q is the deoxyhemoglobin content (dHb) of vein, s is the flow inducing signal (these values are normalized to their values at rest), u is the stimulus function, and y_B is the BOLD signal. The time-varying intrinsic variables f, v, q and s summarize the hemodynamics of the system: how the changes of the CBF, CBV, and dHb are coupled to each other and synaptic activity encoded in the stimulus function u. The other parameters in the above equations are the neural efficiency ϵ, the flow decay k_s, the flow time constant k_f, Grubb's parameter α, the venous transit time τ, the resting net oxygen extraction fraction E_0, and the resting blood volume fraction V_0.

III. Results and Discussion

A. Simulated Data

In this section, the proposed RBF neural network method was first tested on a simple example to validate the estimation accuracy of the Volterra kernels. Then, the simulated BOLD signal (using Balloon model) with different noise levels and real event-related fMRI data were investigated to reconstruct the dynamics underlying the fMRI signal.

1) Example1: In this general example, RBF neural network was applied to the simulated data to identify the coefficients of the Volterra kernels. A total of 400 data points were generated using the following Volterra series model ($P=2$):

$$y(n)=2.4+0.9u(n)-0.4u(n-1)+0.74u(n-2) \\ -0.18u(n-1)u(n-2)+0.36u(n)^2. \quad (27)$$

The input signal $u(n)$ in this example is simulated by Gaussian white noise with unit variance. Fig. 2 shows one realization of the input signal $u(n)$ [Fig. 2(a)] and the simulated output signal $y(n)$ [Fig. 2(b)] using (27).

The RBF neural network with different number of hidden units ($M=50$, 100, 200, 300) (respectively represented as RBF50, RBF100, RBF200, RBF300 in Table I) are investigated. The Bayesian learning procedure described in Section II is applied to regress the output signal $y(n)$ on the input vector $\mathbf{u}(n)$ (From (27), the maximum delay P in the input vector $\mathbf{u}(n)$ is accordingly set to be 2). The M centers of the RBF network basis functions are randomly chosen from the training data set. The estimated Volterra kernels (using (14)–(17)) are shown in Table I. Due to the symmetry of the second-order coefficients ($a_2(i,j)=a_2(j,i)$), we only show the estimated coefficients where $i\le j$. The goodness-of-fit of the RBF neural network with different number of hidden units is evaluated using the normalized mean square error (NMSE) defined as

$$\mathrm{NMSE}=\frac{\sum_{i=0}^{L-1}(\hat{x}_i-x_i)^2}{\sum_{i=0}^{L-1}x_i^2} \quad (28)$$

where $\hat{x}_i$ and x_i are, respectively, the estimated value and the true value of the Volterra kernel parameters.

From Table I, it is clear that although the RBF with small number of hidden units (RBF50) shows some estimation errors (with $\mathrm{NMSE}=0.004$ which is relatively large), the estimation results are accurate when the number of hidden units is large (RBF100, RBF200, and RBF300 with NMSE equal to

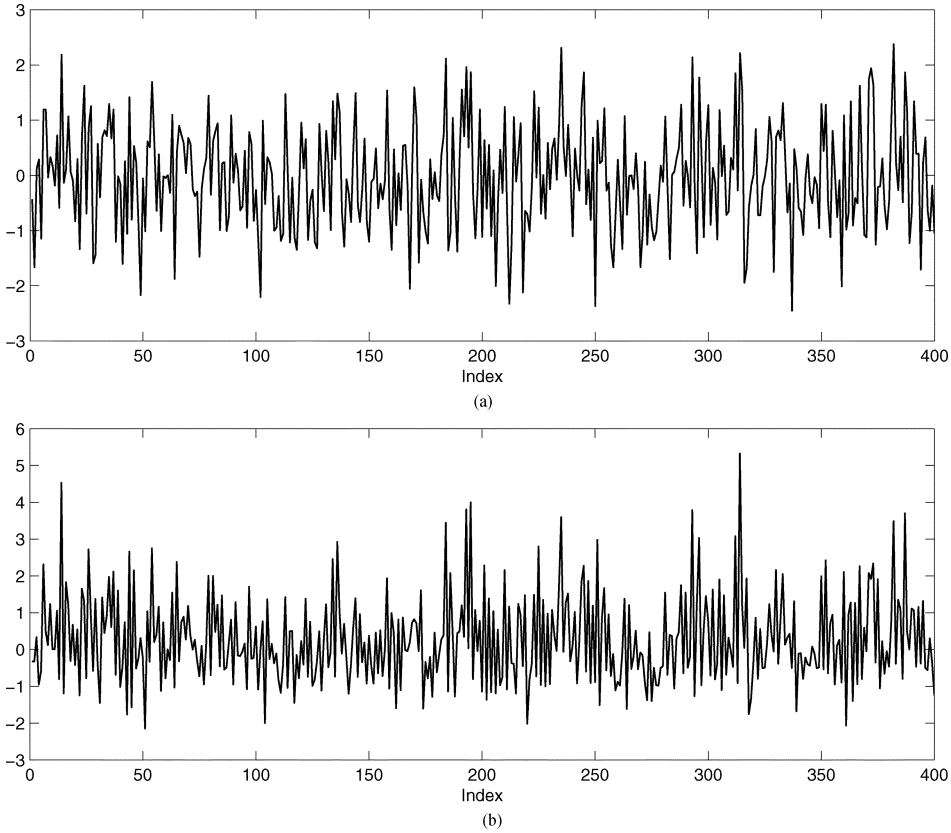

Fig. 2. One realization of the input signal and the simulated output signal using (27). (a) Input signal; (b) Output signal.

TABLE I
ESTIMATION OF VOLTERRA KERNEL PARAMETERS ($P = 2$)

Parameters	Value	RBF50	RBF100	RBF200	RBF300
a_0	2.4	2.4475	2.4062	2.4030	2.4014
$a_1(0)$	0.9	0.8842	0.9207	0.9038	0.9055
$a_1(1)$	-0.4	-0.3511	-0.4169	-0.4020	-0.4017
$a_1(2)$	0.74	0.7157	0.7520	0.7422	0.7423
$a_2(0,0)$	0.36	0.2341	0.3628	0.3592	0.3569
$a_2(0,1)$	0	0.0191	-0.0069	-0.0004	-0.0003
$a_2(0,2)$	0	-0.0076	0.0046	-0.0033	-0.0029
$a_2(1,1)$	0	-0.0619	-0.0092	-0.0015	-0.0010
$a_2(1,2)$	-0.09	-0.0890	-0.0901	-0.0901	-0.0881
$a_2(2,2)$	0	-0.0669	0.0111	-0.0043	-0.0040
NMSE		0.004	1.593e-4	8.728e-6	1.067e-5

$1.593\text{e}{-004}$, $8.728\text{e}{-006}$, and $1.067\text{e}{-005}$ respectively which are relatively small). This study shows that the zeroth, first, and second-order Volterra kernels could be accurately estimated by the proposed method.

2) Example2: To compare the proposed neural network method and Volterra series method using LS estimation, a nonlinear signal with third-order Volterra kernels is generated according to the following equation:

$$\begin{aligned} y(n) = {} & 2.4 + 0.9u(n) - 0.4u(n-1) + 0.74u(n-2) \\ & - 0.18u(n-1)u(n-2) + 0.36u(n)^2 \\ & + 0.76u(n)u(n-1)u(n-2) \\ & + 0.85u(n-1)u(n-2)^2 + e(n). \end{aligned} \tag{29}$$

TABLE II
ESTIMATION OF VOLTERRA KERNEL PARAMETERS USING RBF NEURAL NETWORK METHOD AND LS METHOD WHEN THE HIGHEST ORDER OF VOLTERRA SERIES IS 3

Kernels	Parameters	Value	RBF	LS-2	LS-3
zeroth	a_0	2.4	2.4064	2.1953	2.4006
first	$a_1(0)$	0.9	0.9018	0.8785	0.9013
	$a_1(1)$	-0.4	-0.3888	0.4764	-0.4013
	$a_1(2)$	0.74	0.7480	0.9776	0.7388
second	$a_2(0,0)$	0.36	0.3681	0.4146	0.3596
	$a_2(0,1)$	0	0.0023	0.0252	0.0012
	$a_2(0,2)$	0	0.0158	0.2670	0.0005
	$a_2(1,1)$	0	-0.0008	0.0177	0.0000
	$a_2(1,2)$	-0.09	-0.0840	-0.1943	-0.0895
	$a_2(2,2)$	0	0.0139	0.1340	-0.0001
NMSE			1.0573e-4	0.1309	9.8310e-7

As before, the input signal $u(n)$ is Gaussian white noise with variance one and the total number of data points is 400. In this example, a small Gaussian noise $e(n)$ with variance 0.01 is also added to generate the noisy simulated signal $y(n)$. The maximum delay P in the input vector $\mathbf{u}(n)$ is set to be 2. For the RBF neural network, 200 hidden units ($M = 200$) are used to regress the simulated output signal $y(n)$ to the input signal $u(n)$ in order to have good results. For the LS estimation method, the choice of the highest Volterra kernel order need to be specified. The estimations with the highest assumed order being set to 2 (LS-2) and 3 (LS-3) are examined. Table II shows the estimation results of RBF, LS-2, and LS-3.

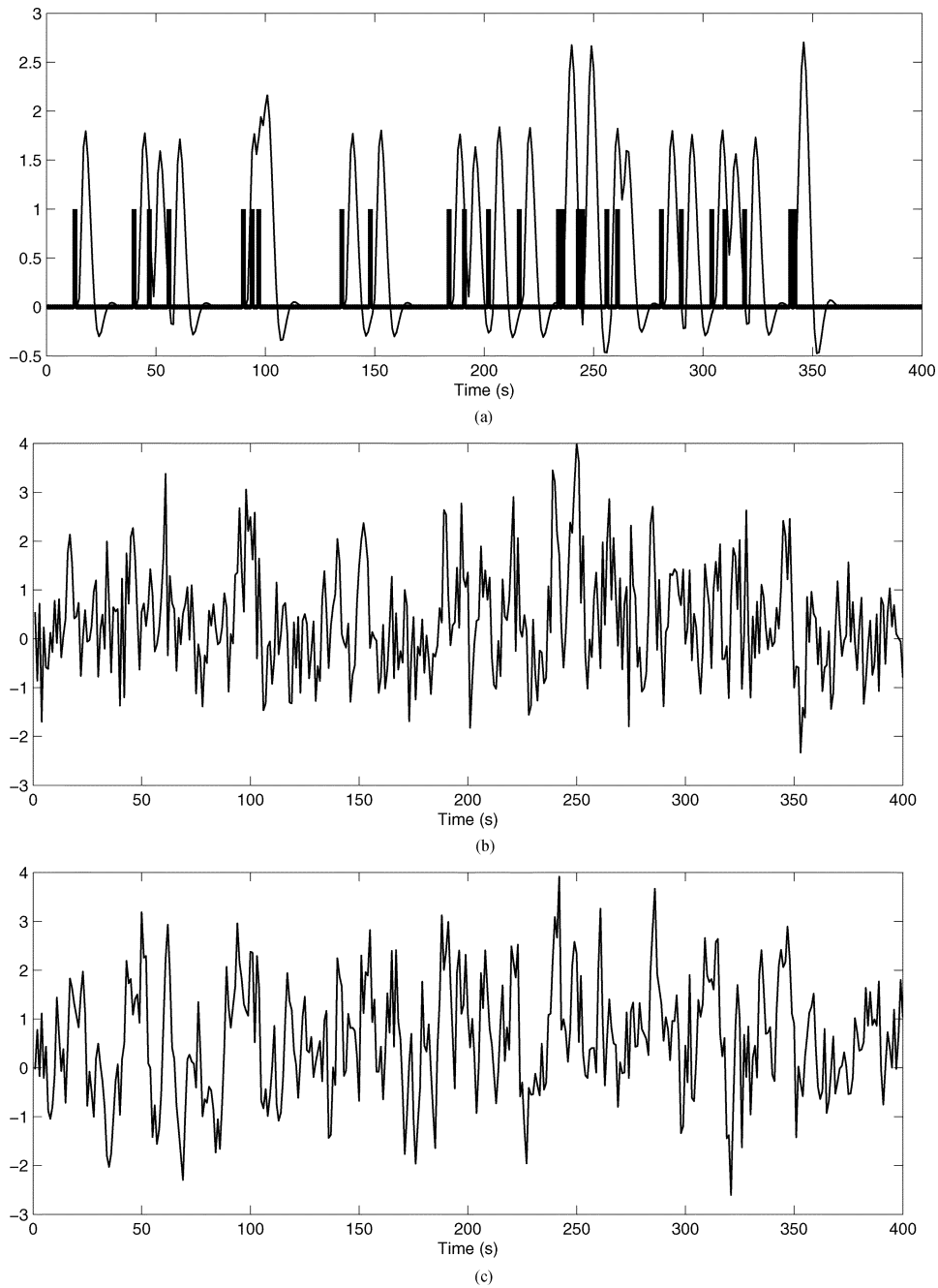

Fig. 3. Simulated BOLD signal generated by the Balloon model and noisy BOLD signals with different additive noise. (a) Simulated pure BOLD signal and the timing of the stimuli; (b) Simulated noisy BOLD signal corrupted with additive Gaussian white noise; (c) Simulated noisy BOLD signal corrupted with additive autocorrelation noise.

From Table II, it is clear that the least-squares estimation is sensitive to the assumption of the highest order of Volterra kernels. If the chosen order mismatches with the actual order, the estimation results may deviate from the true values as shown in the LS-2 with large NMSE (0.1309). Including higher order Volterra kernels into the LS method may result in better estimation [as shown in LS-3 with small NMSE ($9.8310\mathrm{e}{-007}$)], however, this is difficult for fMRI data analysis since the number of parameters to be estimated from LS method may become enormously high with the increasing order of the kernels included. The RBF neural network method, on the other hand, does not rely on the choice of the order and, hence, could accurately estimate the Volterra kernels even if the order of the Volterra series is unknown (with relatively small $\mathrm{NMSE} = 1.0573\mathrm{e}-004$). Another advantage of RBF neural network method is that we can estimate Volterra kernels at a specified order while without estimating Volterra kernels at other orders. Compared to the LS method which needs to estimate all the Volterra kernels together, this property of RBF neural network could estimate the lower order Volterra kernels independently without estimating the higher order kernels. This is efficient because the lower order Volterra kernels are of our interest for most cases.

From the simulation studies on Example1 and Example2, it is shown that the proposed RBF neural network method works well in the general Volterra series models. The estimated Volterra kernels are accurate as long as enough number of

hidden units are used in the network structure. In the following section, a case closer to the fMRI data—the simulated BOLD signal is tested.

3) Simulated Bold Signal: In this set of simulations, the simulated BOLD signal generated using Balloon model is investigated using the proposed RBF neural network method. When RBF neural network is applied to the fMRI data, the noise involved in the fMRI signal may pose a problem. In this section, both the Gaussian white noise and autocorrelation noise in the fMRI data are examined.

The simulated BOLD signal y_B is generated using (26) with the following set of parameters: $\epsilon = 0.5$, $k_s = 0.65$, $k_f = 0.4$, $\tau = 1$, $\alpha = 0.4$, $E_0 = 0.4$ and $V_0 = 0.02$ [14], [15] and the total duration of the simulated BOLD signal is 400 s. To simulate the event-related fMRI experiment, the input stimuli u are randomly generated with each lasting for 1 s. The generated BOLD signal is then sampled with uniform sampling rate of 1 s, which gives the simulated BOLD signal $y_B(n)$. Fig. 3(a) illustrates the simulated BOLD signal $y_B(n)$ with the thick vertical line indicating the timing of the discrete random stimuli $u(n)$.

To test the effectiveness of the proposed method in the case of additive noise, the noise $e(n)$ was added to the BOLD signal $y_B(n)$ generated by the Balloon model as follows:

$$y(n) = y_B(n) + e(n) \tag{30}$$

where $e(n)$ is the additive noise (Gaussian white noise or noise with temporal autocorrelation) and $y(n)$ is the noisy BOLD signal. Then, the simulated input stimuli $u(n)$ were fed to the RBF network with the simulated noisy BOLD signal $y(n)$ as the target signal. The number of hidden units M in the RBF neural network is set to be 200 (enough to model the nonlinearity in the system) and the centers of the RBF are selected randomly from the input stimuli vectors. The parameters of the RBF neural network are estimated through the Bayesian learning. To cover the time span of the HDR, the maximum input delay P is chosen to be 20 since the HDR lasts for about 20 s and the sampling rate is 1 s in this simulation.

Fig. 3(b) shows the simulated noisy BOLD signal $y(n)$ with additive Gaussian white noise. Different noise levels (with the signal-to-noise ratio (SNR) varying from -7 to 5 dB) are added to the simulated BOLD signal $y_B(n)$ to generate the noisy BOLD signal $y(n)$. Figs. 4 and 5 show the the estimated first- (a vector of dimension 21×1) and second-order (a symmetric matrix of dimension 21×21) Volterra kernels of the simulated noisy BOLD signal with the SNR of -7 and 0 dB respectively. It is clear from the figures that the estimated first-order kernel of Volterra series shows the properties of the HDR and is analogous to the conventional HRF formed by the difference of two Gamma functions. When the noise level is high, the estimated HDR exhibits more variations as displayed in Fig. 4(a). The second-order kernels in these figures indicate the effect of the interaction between adjacent inputs on output signal.

Next, the noise with temporal autocorrelation is investigated. The serial correlations in fMRI data is simulated as autoregressive with order 1 (AR(1)) plus white noise [21]

$$e(n) = z(n) + \eta(n) \tag{31}$$

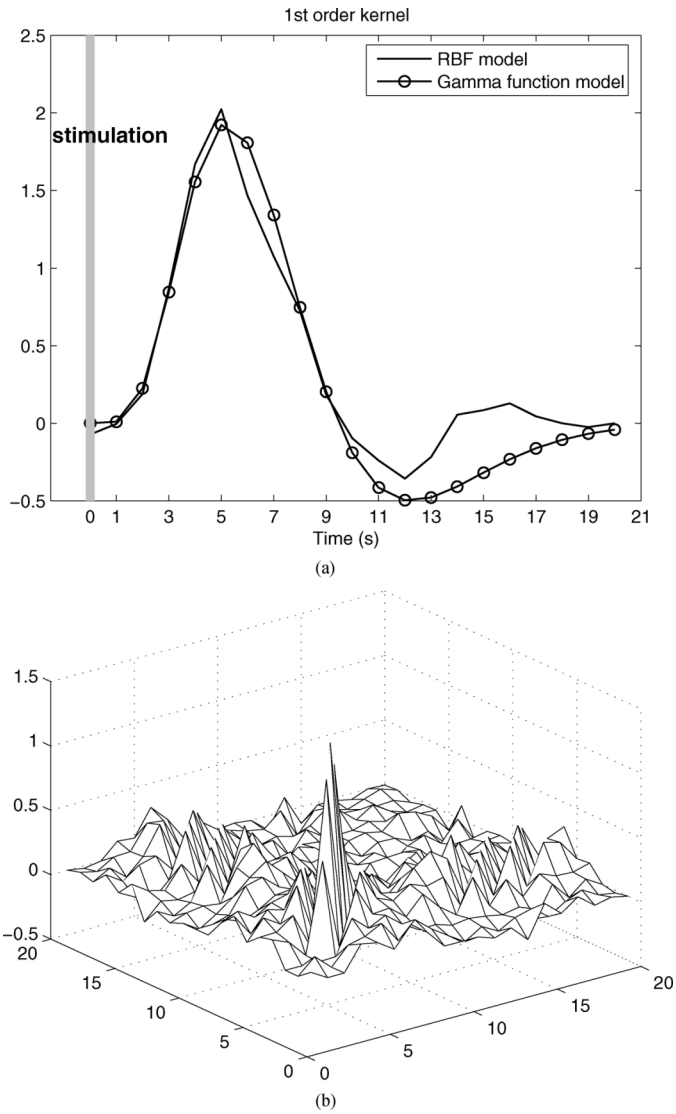

Fig. 5. Estimated first- (a) and second-order (b) Volterra kernels using the proposed neural network method with $\mathrm{SNR} = 0$ dB.

$$z(n) = \rho z(n-1) + \xi(n) \tag{32}$$

where ρ is the AR(1) coefficient, $\eta(n)$ and $\xi(n)$ are the white noise terms ($\eta(n) \sim N(0, \sigma_\eta^2)$, $\xi(n) \sim N(0, \sigma_\xi^2)$). This noise model is to capture the short-range autocorrelations in the fMRI data. For long-range autocorrelations in the fMRI data, a detrend procedure is often included as a preprocessing step to relax the autocorrelation noise [22]. In the following part, the short-range autocorrelation noise is investigated.

The short-range autocorrelation noise synthesized using parameters $\rho = 0.4$ and $\sigma_\eta^2 = 0.5$, $\sigma_\xi^2 = 0.6$ is added to the pure BOLD signal $y_B(n)$ to generate the noisy BOLD signal $y(n)$ as shown in Fig. 3(c). This simulated noisy BOLD signal is then modelled using the RBF neural network. The parameters of the RBF neural network are chosen according to the same scheme as introduced in the case of the Gaussian white noise. Fig. 6 shows the estimated first- and second-order Volterra kernels using the proposed RBF neural network method. These results indicate that the RBF neural network method performs well to estimate the Volterra kernels when the noise is of short-range temporal

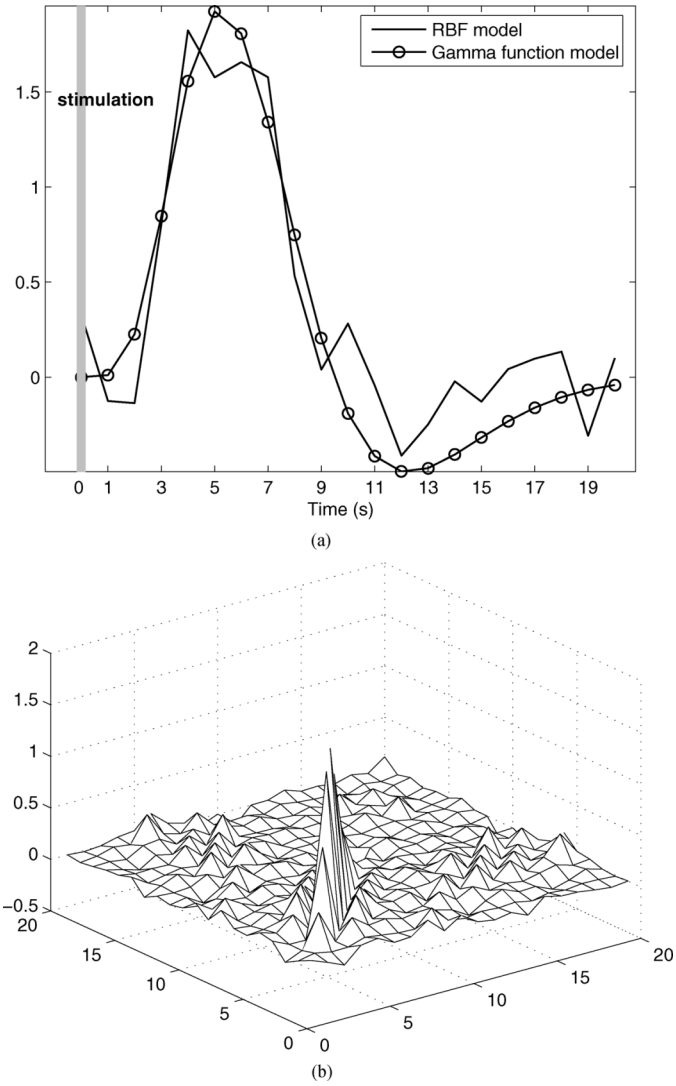

Fig. 4. Estimated first- (a) and second-order (b) Volterra kernels using the proposed neural network method with $\mathrm{SNR} = -7$ dB.

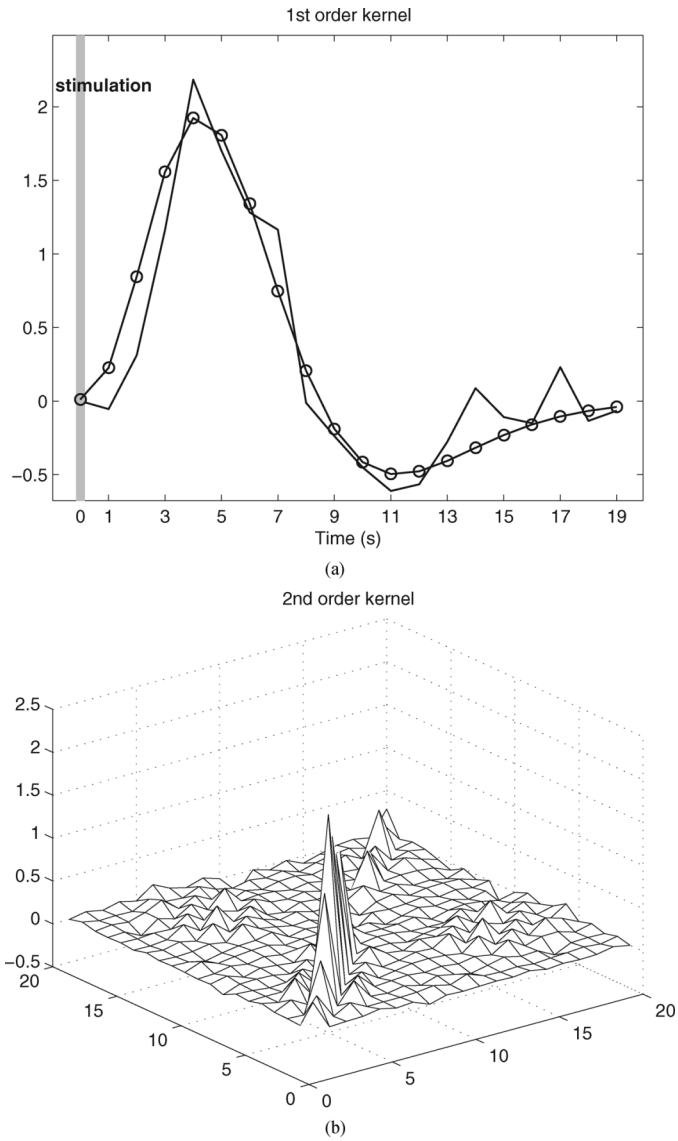

Fig. 6. Estimated (a) first- and (b) second-order Volterra kernels using the proposed neural network method when the additive noise is autocorrelational.

autocorrelation. This shows that the short-range autocorrelation noise is not so problematic for the proposed RBF neural network method. When the noise is of long-range autocorrelation, the performance of the RBF neural network would be affected by the long-range autocorrelation and may not work well. Hence, to ensure that the RBF neural network method works well, the fMRI data need to be detrended before applying the RBF neural network for further processing.

B. Real Data

1) Data Details: The proposed RBF neural network method for the estimation of the hemodynamic response is also tested on a real event-related fMRI data. This real fMRI experiment was designed for detection of visual-mental imagery and perception — transient activity in the human calcarine cortex. The functional data were acquired using echo planar imaging (EPI) with the imaging parameters: $\mathrm{echo\ time(TE)} = 40$ ms, $\mathrm{TR} = 2000$ ms, $\mathrm{flip\ angle} = 90°$, and 64×80 matrix. The details of the experiment can be found in [23]. This data is obtained from the National fMRI data center (http://www.fmridc.org) with the accession number 2–2000–11127. During the experiment, after hearing the name of an animal, the subjects were told to form an image mentally; then, the subjects evaluated the characteristics of the named animal after hearing an auditory instruction of a specific property of the named animal. The total number of data points for this experiment is 308, with several visual-mental processes.

From the description of the experiment, in addition to the visual-mental process, the subjects were also given auditory stimuli, hence, the auditory cortex should also be activated. The auditory stimuli lasting for 2 s are presented with fixed interval and separated 14 s apart (7 scans). In this section, the activation of the auditory cortex is investigated. Before using the proposed neural network method to this real event-related fMRI data, the raw data are preprocessed by the SPM software [8] for registration, normalization and smoothing. The drift (long-range autocorrelation noise) in each voxel time series is removed using

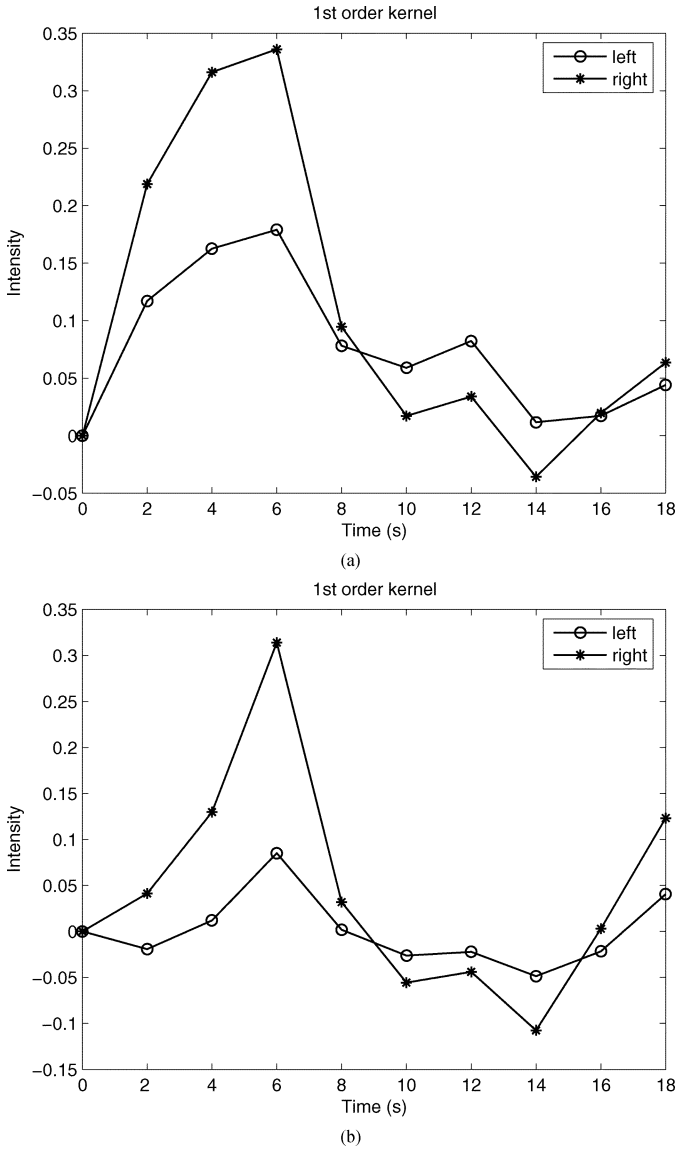

Fig. 7. Estimated first-order Volterra kernels of the left and right auditory cortex for two subjects. (a) Subject 1; (b) Subject 2.

the detrending procedure to ensure the proposed neural network method works well.

The preprocessed fMRI signal is then applied to the RBF neural network with the number of hidden units $M = 200$. The measured fMRI signal at each voxel is used as the desired signal $y(n)$ of the RBF neural network and the input signal $u(n)$ is constructed according to the description of the experimental design. When the stimuli are presented, $u(n) = 1$; while when the stimuli are absent, $u(n) = 0$. Since the sampling rate (TR) is 2 s, the maximum delay P of the input vector is chosen to be 10 in order to cover the time span (20 s) of the HDR.

2) Estimation of HDR: As mentioned in the Introduction section, the HDR varies with different brain regions and different subjects. In this section we examine these variations. Fig. 7 shows the estimated first order Volterra kernels of the left and right auditory cortex for two subjects using the proposed neural network method. Clearly, the variations of the HDR between different brain regions and different subjects can be captured

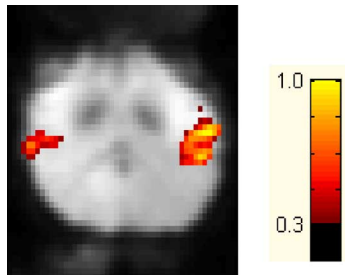

Fig. 8. One slice showing the activation of the auditory cortex ($R > 0.3$).

using the proposed method. The estimated first order Volterra kernels show the properties of the HDR, such as a characteristic peak at around 6 s. The estimated second-order kernels showed the same patterns as that is shown in Fig. 4(b) and, hence, not shown here. These figures illustrate that the proposed neural network method is able to provide a good estimation of the HDR. In addition, it is more flexible than the conventional HDR model formulated by the difference between two Gamma functions. The Gamma function model may miss the difference in the dynamics of different regions and subjects since it uses the same HDR model for all the voxels investigated. However, the proposed neural network method is applied on each voxel and is able to capture the differences in BOLD signals of different regions and subjects.

3) Detection of the Activated Regions: To detect the activated regions of the brain, the reconstructed BOLD signal $\hat{\mathbf{y}}$ at the output of the RBF neural network is investigated. The following test at each voxel is used as an index (R) for activation detection

$$R = \frac{\|\hat{\mathbf{y}}\|}{\|\mathbf{y} - \hat{\mathbf{y}}\|} \tag{33}$$

where $\mathbf{y}$ is the measured fMRI signal in a voxel and $\hat{\mathbf{y}}$ is the reconstructed (or regressed) BOLD signal in this voxel. For the inactivated voxels, the reconstructed BOLD signal would be almost zero since the inactivated voxels do not involve the BOLD effect corresponding to the external stimuli. In this case, the value of R would be small. On the other hand, when the voxel is activated, the reconstructed BOLD signal should capture the dynamics corresponding to the input stimulations, that is, $\hat{\mathbf{y}} \neq 0$ and the value R would be large. The R value is analogous to the SNR. Fig. 8 shows the results of the activated regions in the brain by thresholding the R values at each voxel ($R > 0.3$ is chosen to give best results). It is clear from this figure that the auditory cortex in the brain is activated in this event-related fMRI experiment.

IV. Conclusion

The BOLD signal, as the foundation of the fMRI experiment, reflects the hemodynamic response of human brain. To investigate how the brain responds to the stimulus, i.e., to study the dynamics of the human brain, the system identification methods have been proposed to identify the complex functional relationship between the input stimuli and the measured BOLD signal. Conventional method is based on the linear system analysis which models the BOLD signal as the convolution of the HDR and the input stimuli. However, considering the

nonlinear nature of the BOLD signal, nonlinear methods are preferred for the identification of this complex (brain) system. One of these nonlinear models is the Balloon model which is a physiologically derived one. In this work, the Volterra series, which can represent any dynamical input-state-output system, was first investigated to provide a nonparametric framework for the system identification. Then, the RBF neural network is proposed as a general method to regress the measured BOLD signal on the input stimuli and to capture the system dynamics. The equivalence of the proposed RBF neural network method to the Volterra kernels has been derived. It is demonstrated that the first- and second-order Volterra kernels can be easily deduced from the coefficients of the RBF neural network. Compared to the Volterra series model estimated through least-squares method, the RBF neural network method does not need to presume the highest order of the nonlinear system and, hence, is robust and efficient to estimate the Volterra kernels even when the nonlinear system is of higher order. Results from simulated as well as real event-related fMRI signals show that the proposed method can successfully estimate the HDR as well as capture the nonlinear dynamics of the BOLD signal. In addition, the proposed method could estimate the individual hemodynamic response (or the first-order Volterra kernel) at each voxel. This helps us to investigate the variations of the HDR with different brain regions and different subjects.

REFERENCES

[1] S. Ogawa, T. Lee, A. Nayak, and P. Glynn, "Oxygenation-sensitive contrast in magnetic resonance image of rodent brain of high magnetic fields," *Magn. Reson, Med.*, vol. 14, pp. 68–78, 1990.

[2] P. Jezzard, P. Matthews, and S. Smith, Eds., *Functional Magnetic Resonance Imaging: An Introduction to Methods*. Oxford, U.K.: Oxford Univ. Press, 2001.

[3] S. A. Huettel, A. W. Song, and G. McCarthy, *Functional Magnetic Resonance Imaging*. Sunderland, MA: Sinauer, 2004.

[4] R. B. Buxton, *Introduction to Functional Magnetic Resonance Imaging: Principles and Techniques*. Cambridge, MA: Cambridge Univ. Press, 2002.

[5] K. J. Friston, A. P. Holmes, K. J. Worsley, J. P. Poline, C. D. Frith, and R. S. J. Frackowiak, "Statistical parametric maps in functional imaging: A general linear approach," *Hum. Brain Mapp.*, vol. 2, pp. 189–210, 1995.

[6] G. M. Boynton, S. A. Engel, G. H. Glover, and D. J. Heeger, "Linear systems analysis of functional magnetic resonance imaging in human V1," *J. Neurosci.*, vol. 16, pp. 4207–4221, 1996.

[7] D. A. Handwerker, J. M. Ollinger, and M. D'Esposito, "Variation of BOLD hemodynamic responses across subjects and brain regions and their effects on statistical analyses," *NeuroImage*, vol. 21, pp. 1639–1651, 2004.

[8] R. Frackowiak, K. J. Friston, C. Frith, R. Dolan, C. Price, S. Zeki, J. Ashburner, and W. Penny, Eds., *Human Brain Function*, 2nd ed. New York: Academic, 2003.

[9] R. M. Birn, Z. S. Saad, and P. A. Bandettini, "Spatial heterogeneity of the nonlinear dynamics in the fMRI BOLD response," *NeuroImage*, vol. 14, pp. 817–826, 2001.

[10] A. Laird, B. Rogers, and M. Meyerand, "Investigating the nonlinearity of fMRI activation data," in *Proc. 2nd Joint EMBS/BMES Conf.*, 2002, pp. 23–26.

[11] K. L. Miller, W. M. Luh, T. T. Liu, A. Martinez, T. Obata, E. C. Wong, L. R. Frank, and R. B. Buxton, "Nonlinear temporal dynamics of the cerebral blood flow response," *Hum. Brain Mapp.*, vol. 13, pp. 1–12, 2001.

[12] T. D. Wager, A. Vazquez, L. Hernandez, and D. C. Noll, "Accounting for nonlinear BOLD effects in fMRI: Parameter estimates and a model for prediction in rapid event-related studies," *NeuroImage*, vol. 25, pp. 206–218, 2005.

[13] K. J. Friston, O. Josephs, G. Rees, and R. Turner, "Nonlinear event-related responses in fMRI," *Magn. Reson, Med.*, vol. 39, pp. 41–52, 1998.

[14] R. Buxton, E. Wong, and L. Frank, "Dynamics of blood flow and oxygenation changes during brain activation: The Balloon model," *Magn. Reson. Med.*, vol. 39, pp. 855–864, 1998.

[15] K. J. Friston, A. Mechelli, R. Turner, and C. J. Price, "Nonlinear responses in fMRI: The Balloon model, Volterra kernels, and other hemodynamics," *NeuroImage*, vol. 12, pp. 466–477, 2000.

[16] R. Buxton, K. Uludag, D. J. Dubowitz, and T. T. Liu, "Modeling the hemodynamic response to brain activation," *NeuroImage*, vol. 23, pp. S220–S233, 2004.

[17] S. Haykin, *Neural Networks: A Comprehensive Foundation*, 2nd ed. Upper Saddle River, NJ: Prentice-Hall, 1999.

[18] M. Misaki and S. Miyauchi, "Application of artificial neural network to fMRI regression analysis," *NeuroImage*, vol. 29, pp. 396–408, 2006.

[19] H. Luo and S. Puthusserypady, "NARX neural networks for dynamical modelling of fMRI data," presented at the IEEE World Congr. Computational Intelligence, Vancouver, BC, Canada, Jul. 16–21, 2006.

[20] E. Rank, "Application of Bayesian trained RBF networks to nonlinear time-series modeling," *Signal Process.*, vol. 83, pp. 1393–1410, 2003.

[21] P. L. Purdon and R. Weisskoff, "Effect of temporal autocorrelation due to physiological noise and stimulus paradigm on voxel-level false-positive rates in fMRI," *Hum. Brain Mapp.*, vol. 6, pp. 239–249, 1998.

[22] J. Tanabe, D. Miller, J. Tregellas, R. Freedman, and F. G. Meyer, "Comparison of detrending methods for optimal fMRI preprocessing," *NeuroImage*, vol. 15, pp. 902–907, 2002.

[23] I. Klein, A. Paradis, J. Poline, S. Kosslyn, and D. Bihan, "Transient activity in the human calcarine cortex during visual-mental imagery: An event-related fMRI study," *J. Cogn.Neurosci.*, vol. 12, no. 2, pp. 15–23, 2000.

Huaien Luo received the B.E. and M.E. degrees in electronics and information engineering from Huazhong University of Science and Technology, Wuhan, China, in 2000 and 2003, respectively. He is currently working towards the Ph.D. degree at the Department of Electrical and Computer Engineering, National University of Singapore, Singapore.

His research interests include statistical signal processing, especially biomedical signal processing and data analysis.

Sadasivan Puthusserypady (M'00–SM'05) received the B.Tech. degree in electrical engineering and the M.Tech. degree in instrumentation and control systems engineering from University of Calicut, Kerala, India, in 1986 and 1989, respectively. He received the Ph.D. degree in electrical communication engineering from the Indian Institute of Science, Bangalore, India, in 1995.

During 1993–1996, he was a Research Associate at the Department of Psychopharmacology, NIMHANS, Bangalore, India. He was a Postdoctoral Research Fellow at the Communications Research Laboratory, McMaster University, Hamilton, ON, Canada, from 1996 to 1998. From 1998 to 2000, he was a Senior Systems Engineer at Raytheon Systems Canada Ltd., Waterloo, ON, Canada. He is currently an Assistant Professor at the Department of Electrical and Computer Engineering, National University of Singapore, Singapore. His research interests are in biomedical signal processing, neural networks, and multiuser detection and chaotic communication systems.